Shore Protection Structures on the Coast of Biduk-Biduk District, Indonesia

Tommy Ekamitra Sutarto[a]
Department of Civil Engineering, Politeknik Negeri Samarinda, Jl. Ciptomangun Kusumo, Samarinda, Indonesia

Keywords: Shore Protection Structure, Seawall, Wave Prediction, Fetch, Wave Height, Tide.

Abstract: Biduk-Biduk Beach in Kalimantan Timur Province of Indonesia continues to experience abrasion, while the existing shore protection structures were yet uneffective. In some places, structural failure occurs, even the existing structures had occupied wide space and create aesthetical issues. The purpose of this study was to determine proper sites, type, and design of shore protection structures that meet planning standards such that the structures were stable, effective in controlling abrasion, and in line with the Biduk-Biduk coastal tourism development plan. The study was performed in four stages, namely: 1) the preparation and preliminary survey, 2) the main survey, 3) the data analysis and design, and 4) the drawing stage. Soil mechanics, topography, coastal bathymetry, and tidal surveys were conducted at the properly selected location. The structures were designed following technical standards to withstand extreme waves of 25 year return period. The most suitable type of structure was seawall with core materials of cyclopean concrete (60% concrete and 40% local stone) and surfacial material of 20 cm-thick reinforced concrete slab ($f'c$ = 26.4 MPa). The seawall had front wall slope of 1:1.5. The toe of the seawall was seated 1.8 m below beach floor to avoid failure due to undermining of the toe by waves and currents.

1 INTRODUCTION

Biduk-Biduk is one of the districts within the Berau Regency which is located in the east coast of Kalimantan Timur Province, Indonesia (Figure 1). This district has a shoreline with a length of 67 km (Maryadi et al., 2020) and an area of 3,423 km^2 (BPS, 2020) which is divided into 6 villages (villages). Most of the population works as fishermen, but the district has great potential to develop into a coastal tourism area because of its beautiful beach panorama (Maryadi et al., 2020). In several villages, businesses that support tourism such as motels, restaurants, and tourist boat services have grown in number from year to year.

Unfortunately, there was a problem on the shore of Biduk-Biduk that may disrupt the local community's economy and could interupt the plan for converting the area to be one of coastal tourism areas in Indonesia. In several observation points along the shore from points 1 to 9 (Figure 1), the shoreline has been retreating due to wave-induced abrasion. This phenomenon has threaten the existence of nearby houses (Figure 2a), motels, roads (Figure 2b), and other public facilities (Maryadi et al., 2020). In a periode between 2009 and 2019, the retreat length was 4 to 5 m in Pantai Harapan Village and 5 to 6 m in Biduk-Biduk Village (Maryadi et al., 2020).

Figure 1: Study site: Biduk-Biduk Beach with 9 (nine) observation points.

[a] https://orcid.org/0000-0003-3444-0074

Sutarto, T.
Shore Protection Structures on the Coast of Biduk-Biduk District, Indonesia.
DOI: 10.5220/0010942500003260
In *Proceedings of the 4th International Conference on Applied Science and Technology on Engineering Science (iCAST-ES 2021)*, pages 213-220
ISBN: 978-989-758-615-6; ISSN: 2975-8246

Figure 3: Simple coastal protection structures on the shoreline of Biduk-Biduk: (a) breakwater, b) concrete-ring revetment, c) rock revetment, d) gabion.

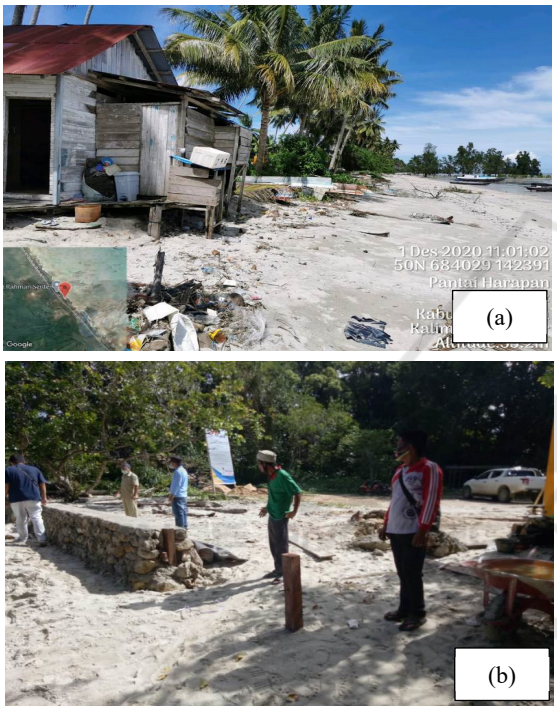

Figure 2: Wave-induced abrasion threaten the exsistence of nearby facilites such as: (a) houses, and (b) roads.

Simple shore protection structures such as breakwater of wood and stone (Figure 3a), concrete-ring revetment (Figure 3b), rock revetment (Figure 3c), and gabion (Figure 3d) were constructed in order to control the rate of abrasion in several locations. However, most of the structures failed to fullfill their functions. In some locations, structural failures can be observed (Maryadi et al., 2020).

Apparently, existing structures were designed based on modest common practices without support from sufficient data and engineering analysis. The breakwaters (Figure 3a) were unstable and experienced frequent overtoping especially during the occurrence of spring tide coincided with strong winds. This condition typically occurs in April. Implementation of concrete-ring revetment (Figure 3b) brought spatial and aesthetic issues into attention when considering future plan for Biduk-Biduk as a tourist destination. Rock revetments (Figure 3c) also experiences frequent overtoping. Instead of absorbing wave energy, these structures created wave reflection capable of eroding the shoreline. Similarly, the existing gabions (Figure 3d) were commonly failed due to corrosion that damaged their wires.

Considering its potential for tourism whereas the existing shore protection structures were not effective, Biduk-Biduk needed a comprehensive shore protection plan that consider site prioritization, suitable type of protection structure, and address the limitations of existing structures. This plan should go along with efforts to preserve mangrove forests which have long been a natural fortress to prevent abrasion on Biduk-Biduk Beach (Prasetyo et al., 2014).

The purpose of this study was to develop a procedure for determining the location, type, and design of effective shore protection structures that fulfilled engineering standards such that those structures were not only effective in controlling abrasion on Biduk-Biduk Beach, but also stable, durable, and in line with local spatial and landuse planning.

2 STUDY SITES

The study sites (Figure 1) were located in Pantai Harapan Village (118.64° E, 1.29° N) and Biduk-Biduk Village (118.72° E, 1.23° N). Both villages are directly adjacent to the Sulawesi Sea. More specifically, the study was focussed on 9 (nine) locations (Figure 1), later called observation points, along the shore. Observation point 1 to 6 were located in Pantai Harapan Village, while the others were in Biduk-Biduk Village.

3 METHODOLOGY

This study was performed in 4 (four) stages, i.e.: 1) preparation and preliminary survey, 2) main surveys, 3) data analysis and detail design, and 4) drawing and reporting. Each stage consisted of several activites as outlined below (Figure 4).

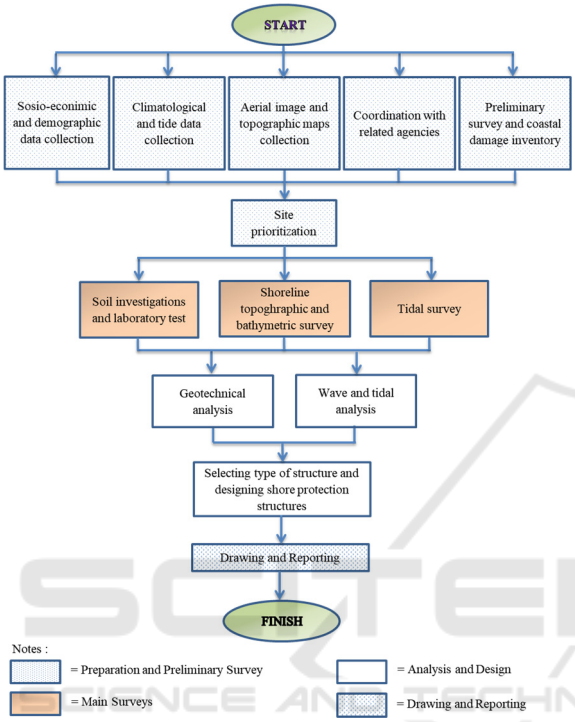

Figure 4: Study procedure.

Preliminary survey was performed by site visits and observing the condition on 9 (nine) observation points (Figure 1). The purposes of preliminary survey was to inventory the condition of available structures including their damages, to identify the locations where intensive abrasion occurred and type of damage it brought to nearby infrastructures, and to discover potential source of construction materials, such as rock quarries, near the location.

The second stage was main surveys. In this stage primary data were obtained through direct measurements, including primary soil data, nearshore topographic map and shore bathymetric data, as well as tidal data. The activites were focused on the selected sites where the structures would be constructed. This stage including 1) soil field and laboratory tests, 2) topographic and bathymetric surveys, and 3) tidal survey. Dutch cone penetration tests were performed to determine the bearing capacity of foundation soils (Figure 5a). Hand boring technique (Figure 5b) was applied to obtain

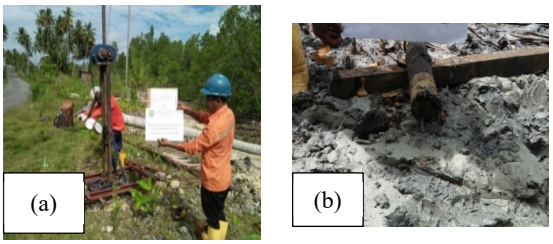

Figure 5: Soil investigation: (a) Dutch cone penetration test, (b) undisturbed soil sampling.

undisturbed soil samples. Topographic measurement was conducted in nearshore zone using real-time kinematic global positioning system (RTK-GPS) (Figure 6a), covered an area with a length of 2000 m and a width of 50 m from the shoreline toward the hinterland. Bathymetric survey was performed side by side with topographic suvey, covered an area with a width of 400 m from the shoreline toward the sea in the shore zone. The bathymetric survey was conducted using echounder GPSMap 580/585 (Figure 6b and 6c).

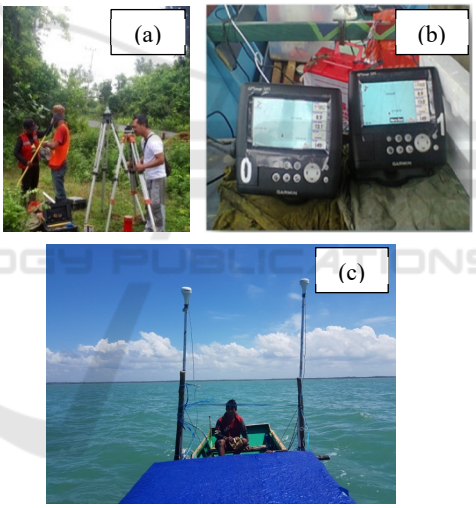

Figure 6: Topographic and bathymetric surveys: (a) GPS Geodetic RTK (b) echosounder GPSMap 580/585, (c) echosounding.

The third stage was analysis and design. In this stage, 4 (four) tasks were performed, i.e. 1) geotechnical analysis, 2) wave and tidal analysis, and 3) selection of suitable type of structure and 4) designing shore protection structures, including determining their construction materials, elevation, and dimensions. All primary and secondary data obtained from previous stages were analysed to obtain required information that would dictate the dimension of structures. A weighted scoring model was developed to help determining the most suitable type of structure for each location.

The last stage in this study procedure was drawing and reporting. The main activities in this stage were to make technical drawings for all the designed structures and to produce study reports that explained all the activites and results obtained in every stage of the study.

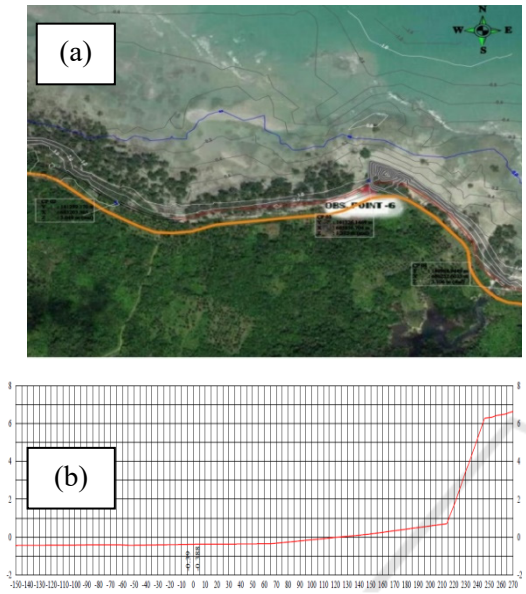

Figure 7: Results of topographic and bathymetric surveys at Pantai Harapan Village (point 6): (a) contour, (b) typical cross-shore profile

4 RESULTS AND DISCUSSION

4.1 Shore Topography and Nearshore Bathymetry

Topographic and bathymetry measurements were performed on the shore and nearshore zone in Pantai Harapan Village (observation point 6). Topographic measurement was conducted 50 m from shoreline toward hinterland using real-time kinematic global positioning system (RTK-GPS) (Figure 6a), while bathymetry measurement was performed 400 m from the shoreline toward the sea using echosounder GPSMap 580/585 (Figure 6b and 6c). The contour map for the measured area in shore and nearshore zones were presented in Figure 7a. Also a typical cross-shore profile could be seen in Figure 7b. The beach slope was typically mild, ranging from 1 to 3 %. The beach slope was typically mild, ranging from 1 to 3 %. Beach material composition was dominated by white fine sand with less coarse sand. A little portion of coral reef fragments were also found in some locations. Typically, beach sediments originate many miles inland where upland and riverbank erosions produce sediments (Papanicolaou, et al., 2014; Sutarto, 2015, 2018, 2020) that were supplied to the beach by streams and rivers. When these sediments reached the shore, they were transported alongshore by waves and current. However, on the shore of Biduk-Biduk, the beach sediments were most probably derived from erosion of coastal formation caused by waves and currents.

4.2 Tide

Biduk-Biduk beach experienced semi-diurnal tide cycle with two high and two low tides of aproximately equal size every lunar day. The most prominent spring tide occurred on March 31 in new moon phase. The high water spring (HWS) was at 1.55 m (msl) and the low water spring (LWS) was at -1.46 (MSL) with mean sea level (MSL) as a datum +0.00 m.

4.3 Fetch Length, *F*

The fetch map for Biduk-Biduk Beach was presented in Figure 8. The winds from the north, north-east, east, south-east, and north-west were prominent in generating wave on Biduk-Biduk Beach. The effective fetch lengths, at any prominent wind direction, were determined for Biduk-Biduk Beach. The results were presented in Table 1.

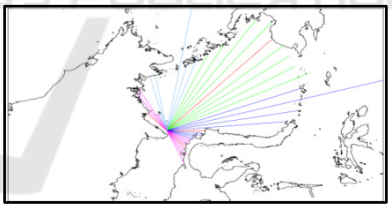

Figure 8: *Fetch* map for Biduk-Biduk Beach.

Table 1: Effective *fetch*.

Wind direction	Effective fetch, F (m)	(km)
North	332,220	332.22
North East	764,628	764.63
East	959,880	959.88
South East	154,317	154.32
North West	101,653	101.65

4.4 Wave Height, *H*, and Period, *T*, in Deep Water

The wave, in this case, refered to the sea wave generated by wind blowing over the sea (Van

Table 2: Calculation of wave height, H, and wave period, T, in deep water.

Year	[a] $U_{L(10)}$ (m/det)	Wind Direction	F (m)	[b] R_L	[c] U_w (m/s)	[d] U_A (m/det)	[e] H (m)	[f] T (s)
2011	2.06	NE	764,628	1.75	3.61	3.44	1.54	8.60
2012	3.09	NE	764,628	1.65	5.10	5.27	2.35	9.92
2013	3.09	NE	764,628	1.65	5.10	5.27	2.35	9.92
2014	3.09	N	332,220	1.65	5.10	5.27	1.55	7.51
2015	3,09	N	332,220	1.65	5.10	5.27	1.55	7.51
2016	3.09	N	332,220	1,65	5.10	5.27	1.55	7.51
2017	4.12	N	332,220	1.50	6.18	6.67	1.96	8.13
2018	3.09	N	332,220	1.65	5.10	5.27	1.55	7.51
2019	3.09	N	332,220	1.65	5.10	5.27	1.55	7.51
2020	4.64	NE	764,628	1.45	6.73	7.41	3.31	11.11

[a] Maximum wind speed $U_{L(10)}$ obtained from weather station in Kalimarau Airport, Berau.

[b] R_L determined based on U_L versus R_L curve (CERC, 1984, p. 3.31).

[c] U_w calculated using equation (1).

[d] U_a calculated using equation (2).

[e] H calculated using equation (3).

[f] T calculated using equation (4).

Vledder and Akpinar, 2015; Chun and Suh, 2019). Its height and period were dictated by a combination of three variables, namely, wind speed, wind duration, and fetch.

Table 2 presents the calculation of wave height, H, and wave period, T, in deep water. The wind speed data were used as input. These data were obtained from the nearest weather station in Kalimarau Airport, Berau for a period from 2011 until 2020 (see column 2 Table 2). The R_L value was determined based on U_L versus R_L curve available in Shore Protection Manual (CERC, 1984). The U_w and U_A values were calculated using equation (1) and (2), respectively. Later, the H and T values could be approximated using equation (3) and (4), successively.

$$U_w = R_L U_{L\,(10)} \quad (1)$$

$$U_A = 0.71(U_w)^{1,23} \quad (2)$$

$$H = 1.6 \times 10^{-3} \frac{{U_A}^2}{g} \left(\frac{gF}{{U_A}^2}\right)^{1/2} \quad (3)$$

$$T = 2.857 \times 10^{-1} \frac{U_A}{g} \left(\frac{gF}{{U_A}^2}\right)^{1/3} \quad (4)$$

4.5 Design-wave Height, H_o, and Period, T_o

A 25-year wave coresponded to the design wave by which the dimensions of shore protection structure were determined. The design-wave height, H_o, was equal to the 25-year wave height, H_{25}, which was obtained from statistical analysis of long-term extreme wave hindcast.

In this case, a frequency distribution analysis was performed for 10 (ten) wave-height data from 2011 until 2020 presented in Table 2. Using Smirnov-Kolmogorov test, it was found that frequency distribution of wave-height best fitted Gumbel distribution as shown in Figure 9, and the 25-year wave height, H_{25}, was equal to 3.61 m (Figure 9). Accordingly, the design wave height, H_o, was equal to 3.61 m. By substituting H_o = 3.61 m and F = 764.628 m (the longest fetch) into equation (3) and (4), the value of design-wave period, T_o, was found and it was equal to 11.44 seconds.

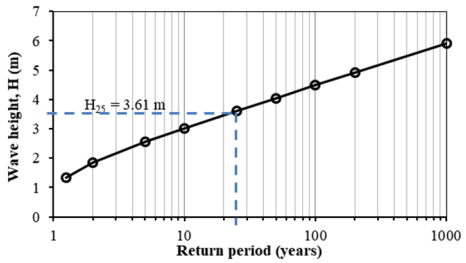

Figure 9: Wave-height frequency distribution follows Gumbel distribution.

4.6 Suitable Type of Structure

Three different types of structure, namely, rock revetment, cyclopean seawall, and concrete or rock

armoured breakwater had the potential to be selected as the most suitable type of structure.

Further assessment were performed using a weighted scoring model to select the most suitable one out of those three alternative structures especially for the location denoted as observation point 6 in Pantai Harapan Village. Cyclopean seawall was the most appropriate type of structure for the location named as observation point 6 in Pantai Harapan Village.

The cyclopean seawall could address the limitation of the available concrete-ring revetment on the site. In contrast to the revetment, the seawall occupied less space and could be designed not to experience overtopping (US Army Corps of Engineers, 2011) even in certain extrem event, for instance, a 25-year wave. Also, seawall was more preferable than breakwater with respect to construction cost, ease of construction, simplicity in repairment, and availability of construction material.

4.7 Seawall Design

For design purpose, the following data, obtained from previous survey and analysis, were summarized here. High Water Spring (HWS) = +1.55 m (MSL), Mean Sea Level (MSL) = +0.00 m, Low Water Spring (LWS) = -1.46 m (MSL), beach slope, m = 0.033 (Figure 7b), design-wave height, H_o= 3.61 m (25-year wave), design-wave period, T_o = 11.44 seconds, dan beach floor elevation = +0.8 (MSL) (Figure 7b).The core material for the seawall was cyclopean concrete consisted of 60% concrete and 40% local stone, while the surfacial material was 20 cm-thick reinforced concrete slab (*f'c* = 26.4 MPa) (Figure 10).

4.7.1 Design-wave Length in Deep Water, L_0

Design-wave length in deep water, L_0 , was approximated by the following formula (Triatmodjo, 2011):

$$L_0 = 1.56\,(T_o)^2 \qquad (5)$$

Substituting T_o = 11.44 m into equation (5) gave L_0 = 204.16 m.

4.7.2 Equivalent Wave Height in Deep Water, H'_0

Taking into account the wave refraction, the equivalent wave height in deep water, H'_0, was approximated using the following formula:

$$H'_0 = K_r H_o \qquad (6)$$

where K_r was refraction coefficient. Substituting K_r = 0.95 and H_o = 3.61 m into equation (6) gave H'_0 = 3.43 m.

4.7.3 Breaking Wave Height, H_b

Breaking wave height, H_b , could be determined using a relation curve for $\frac{H_b}{H'_0}$ and $\frac{H'_o}{gT_0^2}$ provided in Shore Protection Manual Volume II (CERC, 1984, p. 7.7). Previous computation gave H'_0= 3.43 m and T_0 = 9.36 seconds, thus $\frac{H'_0}{gT_0^2} = \frac{3{,}43}{9{,}81 \times 9{,}36^2} = 0.004$. Using the relation curve (for m = 0.033) gave $\frac{H_b}{H'_0} = 1.23$, and $H_b = 1.23H'_0 = 4.22$ m.

4.7.4 Water Depth Corresponding to Breaking Wave, d_b

Similarly, the water depth, d_b, at which the wave start to break, could be determined using a relation curve for $\frac{d_b}{H_b}$ dan $\frac{H_b}{gT_0^2}$ provided in Shore Protection Manual Volume II (CERC, 1984, p. 7.6). Given H_b= 4.22 m and T_0 = 9.36 seconds, then $\frac{H_b}{gT_0^2} = \frac{4{,}22}{9{,}81 \times 9{,}36^2} = 0.0049$. Using the relation curve (for m = 0.033) gave $\frac{d_b}{H_b} = 1.08$, accordingly d_b = 4.58 m.

The condition when $d_b > d_{HWS}$ it signifies the wave had broken before reaching the structure. The water depth near the structure, d_{HWS}, could be determined by substracting HWS level with beach floor level, or d_{HWS} = 1.55 – (+0,80) = 0.75 m. Accordingly, $d_b > d_{HWS}$, this means the wave had broken before reaching the structure.

4.7.5 Near-structure Wave Height, $H_{b\,wall}$

The water depth near the toe of the structure, d_s, could be computed as $d_s = d_{HWS}$ = 0.75 m. Given T_0 = 9.36 seconds and d_s = 0.75 m and using the relation curve for $\frac{H_{b\,wall}}{d_s}$ dan $\frac{d_s}{gT_0^2}$ which was available in Shore Protection Manual Volume II (CERC, 1984, hal. 7.10), the maximum height of the maximum height of wave that reached the structure, $H_{b\,wall}$, could be determined. First, calculate $\frac{d_s}{gT_0^2} = \frac{0{,}75}{9{,}81 \times 9{,}36^2} = 0.0008$. Use the relation curve (for m= 0.033) to obtain $\frac{H_{b\,wall}}{d_s} = 1.13$. Thus, $H_{b\,wall}$ = $1.13d_s$ = 1.75 m.

4.7.6 Wave Runup Height, R_u

The seawall had inclining front wall, also called seaward slope, covered with impermeable surfacial layer of 20 cm-thick reinforced concrete slab (*f'c* = 26.4 MPa) (Figure 10). The seaward slope had an angle, ∅, of 33.69 degrees (above horizontal) or a slope of 1:1.5. This slope would affect the height of wave runup on the seawall, R_u, and frequency of overtopping. Steeper slope would result in less frequent overtopping (Orimoloye et al., 2013; Huang et al., 2020).

For determining the value of R_u, first, calculate Irribaren number using the following equation (Triatmodjo, 2011):

$$I_r = \frac{\tan \emptyset}{(H_{b\,wall} / L_0)^{0,5}} \quad (7)$$

Previous analysis gave $H_{b\,wall}$ = 1.75 m, L_0 = 204,16 m, and ∅ = 33.69 degrees. Substituting these values into equation (7) resulted in I_r = 7.50. Next, plot I_r = 7.50 on the relation curve of I_r versus $\frac{R_u}{H_{b\,wall}}$ (Triatmodjo, 2011, p. 191) that gave $\frac{R_u}{H_{b\,wall}} =$ 2.0. Thus $R_u = 2H_{b\,wall}$ = 2.0 x 1.75 = 3.5 m.

Wave return wall was positioned directly at the top of the seaward slope (Figure 10). This curved wall would effectively block the wave runup such that the runup height could be reduced by half. Accordingly, R_u= 3.5/2 = 1.75 m.

Previous analysis gave $H_{b\,wall}$ = 1.75 m, L_0 = 204,16 m, and ∅ = 33.69 degrees. Substituting these values into equation (8) resulted in I_r = 7.50. Next, plot I_r = 7.50 on the relation curve of I_r versus $\frac{R_u}{H_{b\,wall}}$ (Triatmodjo, 2011, p. 191) that gave $\frac{R_u}{H_{b\,wall}} =$ 2.0. Thus $R_u = 2H_{b\,wall}$ = 2.0 x 1.75 = 3.5 m.

Wave return wall was positioned directly at the top of the seaward slope (Figure 10). This curved wall would effectively block the wave runup such that the runup height could be reduced by half. Accordingly, R_u= 3.5/2 = 1.75 m.

4.7.7 Seawall Crest Level

The seawall was designed not to allow overtopping by extrem waves or design waves of 25-year return period. Therefore, a free board of 0.3 m was added to the height of the seawall. Accordingly, the seawall crest level, El_{crest}, could be determined using the following equation:

$$El_{crest} = HWS + R_u + free\ board \quad (8)$$

Substituting HWS = 1.55 m, R_u = 1.75 m, and free board = 0.3 m into equation (8) gave El_{crest} = +3.60 m (Figure 10).

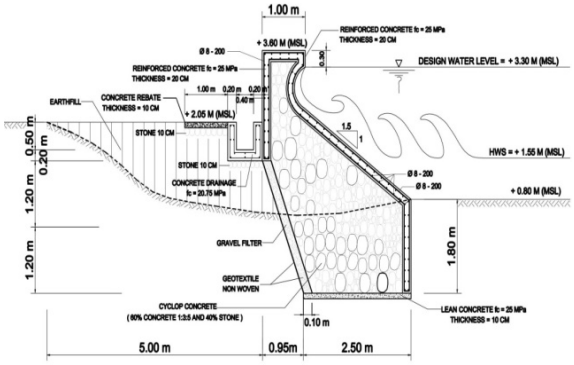

Figure 10: Seawall design for the location denoted as observation point 6 in Pantai Harapan Village.

5 CONCLUSIONS

Cyclopean seawall was the most appropriate type of structure for Biduk-Biduk Beach, most specifically, the location named as observation point 6 in Pantai Harapan Village. The cyclopean seawall could address the limitation of the available concrete-ring revetment on the site. In contrast to the revetment, the seawall occupied less space and could be designed not to experience overtopping (US Army Corps of Engineers, 2011) even in certain extrem event, for instance, a 25-year wave. Also, seawall was more preferable than breakwater with respect to construction cost, ease of construction, simplicity in repairment, and availability of construction material.

The core material for the seawall was cyclopean concrete consisted of 60% concrete and 40% local stone, while the surfacial material waovers 20 cm-thick reinforced concrete *slab* (*f'c* = 26.4 MPa). The seawall had inclining front wall, also called seaward slope, that had a slope of 1:1.5. Wave return wall was positioned directly at the top of the seaward slope to block the wave runup and avoid overtopping. The toe of the seawall was seated 1.8 m below beach floor to avoid failure due to undermining of the toe by waves and currents.

ACKNOWLEDGEMENTS

This study was part of a project entitled: Review Design of Biduk-Biduk Shore Protection Structures funded by Office of Public Works and Public Housing, Kalimantan Timur, Indonesia under contract No. 602/Bid-SDA/KPA/979.J/XI/2020.

REFERENCES

Coastal Engineering Research Center (CERC). (1984). *Shore Protection Manual*, Department of the Army Waterways Experiment Station Corp of Engineers, Vicksburg, Mississippi.

Chun, H., dan Suh, K.D. (2019). Empirical formulas for estimating maximum wave height and period in numerical wave hindcating model, *Ocean Engineering*, No. 193.

Huang, C.-J., Chang, Y.-C., Tai, S.-C., Lin, C.-Y., Lin, Y.-P., Fan, Y., Chiu, C.- M., Wu, L.-C., (2020). Operational monitoring and forecasting of wave run-up on seawalls, *Coastal Engineering*, doi: https://doi.org/10.1016/j.coastaleng.2020.103750.

Maryadi, Setyasih, I., Anwar, Y. (2020) . Efektivitas bangunan pemecah gelombang dalam pengendalian abrasi pantai di Kecamatan Biduk-Biduk, *Jurnal geoedusains*, No.2, Vol. 1, 107-119.

Orimoloye, S., Horrillo-Caraaballo, J., Karunarathna, H., Reeve, D. E. (2020), Wave overtopping of smooth impermeabel seawalls under Unidirectional Bimodal Sea Conditions, *Coastal Engineering*, doi: https://doi.org/10.1016/j.coastaleng.2020.103792.

Papanicolaou, A.N.T., Sutarto, T., Wilson, C.G., Langendoen, E.J. (2014). Bank stability analysis for fluvial erosion and mass failure. In: Proceedings of the 2014 World Environmental and Water Resources Congress, 2014, pp. 1497–1508.

Prasetyo, D.E., Atmanegara, F.K., Zulfikar, F., Purwanti, H.S., Sahri, A., Budiayu, A., dan Sudiono, E. (2014). Kajian sosio-ekologis kawasan mangrove di Pesisir Pantai Kecamatan Biduk-Biduk, Kalimantan Timur, Omni-Akuatika, No.18, Vo.13, 1-9.

Sutarto, T.E. (2015). A combined flume-imaging technique for measuring fluvial erosion of cohesive stream bank soils, *Procedia Engineering*, Vol.125, pp. 368–375.

Sutarto, T.E. (2018) A short review on various techniques for measuring stream bank soil erosion strength, *2018 International Conference on Applied Science and Technology (iCAST)*, pp. 252-258, doi: 10.1109/iCAST1.2018.8751560.

Sutarto, T.E. (2020), Low amplitude of streambank erosion: Distinguishing mass and surface fluvial erosions, *IOP Conference Series: Earth and Environmental Science*, No. 1, Vol. 451, 012093.

Triatmodjo, B. (2011). *Perencanaan Banguan Pantai*, Beta Offset Yogyakarta, Yogyakarta.

US Army Corps of Engineers, 2011, Coastal Engineering Manual-Part VI, Washington D.C.